

Article

Differential Impact of Hexuronate Regulators ExuR and UxuR on the *Escherichia coli* Proteome

Tatiana A. Bessonova^{1,a}, Maria S. Fando^{2,a}, Olga S. Kostareva^{2,a}, Maria N. Tutukina^{1,3,4,a,*}, Olga N. Ozoline¹, Mikhail S. Gelfand^{3,4}, Alexey D. Nikulin² and Svetlana V. Tishchenko²

- ¹ Institute of Cell Biophysics Russian Academy of Sciences PSCBR RAS, Institutskaya, 3, Pushchino, 142290, Russia ; tatianabessonova66@gmail.com, ozoline@rambler.ru
² Institute of Protein Research Russian Academy of Sciences, Institutskaya, 4, Pushchino, 142290, Russia; fando@vega.protres.ru, nikulin@vega.protres.ru, sveta@vega.protres.ru
³ Skolkovo Institute of Science and Technology, Bolshoy Boulevard 30 build 1, Moscow, 121205, Russia; m.tutukina@skoltech.ru, mikhail.gelfand@gmail.com
⁴ Institute for Information Transmission problems Russian Academy of Sciences, Bolshoy Karetny per 19 build 1, Moscow, Russia; m.tutukina@skoltech.ru, mikhail.gelfand@gmail.com
^a These authors share their first joint authorship.
* Correspondence: m.tutukina@skoltech.ru

Abstract: ExuR and UxuR are paralogous proteins belonging to the GntR family of transcriptional regulators. Both are known to control hexuronic acid metabolism in a variety of Gammaproteobacteria but the relative impact of each of them is still unclear. Here, we apply 2D difference electrophoresis followed by mass-spectrometry to characterise the changes in the *Escherichia coli* proteome in response to the *uxuR* or *exuR* deletion. Our data clearly show that the effects are different: deletion of *uxuR* resulted in significantly enhanced expression of D-mannonate dehydratase UxuA and flagellar protein FliC, and inhibition of outer membrane porin OmpF, while the absence of ExuR did not significantly alter the spectrum of detected proteins. This suggests that the roles of proteins predicted as homologs are far from identical.

Effects of *uxuR* deletion were largely dependent on the cultivation conditions: during growth with glucose, UxuA and FliC were dramatically altered, while during growth with glucuronate activation of both was not so prominent. During growth on glucose, the maximal activation was detected for FliC. This was further confirmed by expression analysis and physiological tests thus suggesting involvement of UxuR in the regulation of bacterial motility and biofilm formation.

Keywords: UxuR; ExuR; Ashwell pathway; *uxuAB*; *fliC*; proteome; motility; biofilm formation

1. Introduction

Transcription factors control many steps of a bacterial life cycle, and operate most metabolic switches that take place in *Escherichia coli*. In *E. coli* and closely related proteobacteria, hexuronic acids are utilised via the Ashwell pathway mediated by the two local regulators, UxuR and ExuR. These proteins are paralogous, as the *exuR* gene resulted from duplication of *uxuR* [1]. Together, they control genes encoding all key enzymes for hexuronate utilisation, specifically, oxidoreductase UxuB and mannonate dehydratase UxuA, glucuronidase UidA, glucuronate/galacturonate isomerase UxaC, hexuronate transporters ExuT and GntP, and glucuronide transporters UidB and UidC. Besides, both regulators serve as autorepressors [1-12]. Initially, UxuR was believed to be responsible for all enzymes and transporters related to glucuronate metabolism [5,7,9], while ExuR - for galacturonate metabolism [2,3,6,7]. Later, ExuR and UxuR were shown to cross regulate each other targets, probably forming heterodimers [10-11]. Interchangeability of D-galacturonate and D-glucuronate as effectors and heterodimer formation was further confirmed in [12]. As such, we proposed that the role of ExuR might be in the depression of UxuR-repressed genes via formation of the UxuR-ExuR heterodimer [12].

Several studies suggested that hexuronate metabolism could be important for the ability of proteobacteria to move and to colonise a host intestine [13-15]. Virulence and intestinal colonisation of *Citrobacter rodentium* and enterohaemorrhagic *E. coli* (EHEC) are regulated by the diet-derived galacturonic acid acting via ExuR [16]. However, there is no direct evidence of involvement of UxuR, a key regulator of hexuronate metabolism in *E. coli* K-12 MG1655, in modulation of bacterial motility and colonisation.

Modern transcriptomics can identify RNA-targets of the studied transcription factors, but the resulting levels of proteins may be not proportional to concentrations of the respective mRNAs due to, e.g., differences in the translation rates or protein degradation. Thus, proteomics approaches, in addition to other omics, are useful to evaluate cellular response to deletion of a particular gene, or to a change in growth conditions (for example, a different carbon source). The most popular way to compare proteome maps of the two strains or one strain grown in two different conditions is two-dimensional difference gel electrophoresis (2D DIGE or DIGE), a modification of the 2D electrophoresis where two or three samples are compared on one gel, using varieties of cyan dyes that attach covalently to free amino groups of lysines. This improves reproducibility of experimental data and simplifies identifying differences in the studied proteomic maps.

Here, we use DIGE to investigate changes occurring in the *E. coli* proteomes in response to a deletion of genes encoding regulators of hexuronate metabolism, ExuR and UxuR, during growth on different carbon sources. To prove the detected effects we test expression of genes encoding the most influenced proteins and check the ability of the wild type and its *uxuR* deletion derivative to move and to form biofilms.

2. Results

***exuR* deletion did not influence the proteome of *E. coli* K-12 MG1655**

Surprisingly, the proteomic maps of the wild type *E. coli* K-12 MG1655 and its $\Delta exuR$ derivative did not differ in the spectrum of proteins, both in the cells growing with D-glucose (Figure 1A), and with D-glucuronate (Figure 1B).

This was from one side rather unexpected since ExuR was predicted as a regulator of hexuronate metabolism with a function similar to that of UxuR [1, 7]. From the other, it is in agreement with our previous qRT-PCR and β -galactosidase data where the effects of *exuR* deletion on its predicted targets were moderate [12].

Effects of *uxuR* deletion on the proteome of *E. coli* K-12 MG1655

Unlike the previous case, the comparison of the proteomic maps of the wild type *E. coli* K-12 MG1655 and *E. coli* K-12 MG1655 $\Delta uxuR$ revealed several proteins with significantly changed levels. Rather predictably, these proteins were different during growth on D-glucose (Figure 2A and Table 2) and D-glucuronate (Figure S2 and Table 3).

Figure 2 demonstrates that the proteins most strongly affected by the *uxuR* deletion are D-mannonate dehydratase UxuA, the key enzyme of the Ashwell pathway, and a structural protein of bacterial flagella FliC. The latter showed a dramatic increase suggesting UxuR involvement in regulation of bacterial motility. Changes in concentration of these proteins during growth with D-glucuronate were much less dramatic (Supplementary Figure S2 and Table 3), that could be explained by derepression of the UxuR-mediated genes by ExuR-UxuR heterodimers in the presence of this substrate. Porin OmpF was inhibited in the *uxuR* deletion derivative independent of the carbon source. This might indicate that UxuR plays a role in constitutive regulation of this transport system. Other proteins with altered levels were related to several metabolic pathways, and, interestingly, to a nitrogen metabolism, as UxuR repressed expression of transcriptional regulator NsrR. Changes in the protein spectrum of the wild type cells during growth with glucuronate are shown in Supplementary Figure S3 and Supplementary Table 1. In brief, all major changes were predictably related to metabolic

enzymes and transporters, as well as proteins related to nitrosative and osmotic stress, probably reflecting stress conditions induced by a very poor medium.

Effects of *uxuR* deletion on motility of *E. coli* K-12 MG1655

To check whether UxuR has an effect on bacterial motility, we measured the mobility zones of the wild type strain and its $\Delta uxuR$ derivative during growth with addition of D-glucose or D-glucuronate (Figure 3A).

After 6 hours of growth at 37°C, the motility zones were much larger in the *uxuR* mutant, and this effect was less pronounced in the presence of D-glucuronate. This observation is in line with the DIGE result and suggests that UxuR controls *E. coli* motility in an effector-dependent manner.

To further check this assumption, we measured expression of *fliC* in the wild type K-12 MG1655 and its *exuR* and *uxuR* deletion mutants during growth on D-glucose or D-glucuronate as a sole carbon source. Figure 3B shows that indeed *uxuR* deletion resulted in approximately 30-fold activation of *fliC* during growth on glucose. D-glucuronate impaired this effect, and *exuR* deletion led to only insignificant changes in the *fliC* expression.

Effects of *uxuR* deletion on the biofilm formation of *E. coli* K-12 MG1655

Inhibition of bacterial motility by UxuR highlights the importance of the Ashwell pathway for colonisation of host organisms. The colonisation processes are normally accompanied by formation of bacterial biofilms that help bacteria to survive in harsh conditions. Figure 4 illustrates the influence of *uxuR* deletion on the relative intensity of biofilm formation. As expected, UxuR is necessary for effective generation of biofilms, especially during growth on rich LB medium (Figures 4 A and B).

During growth on minimal medium with glucose the effect of UxuR was much less statistically significant (Figure 4A). We observed that even on one plate two neighbouring wells can yield opposite results, and even the descendants of one colony may show different behaviour (Supplementary Figure S4). We saw the same pattern on DIGE, as in some experiments no FliC activation was detected (an example is shown in Supplementary Figure S1). This might hint at an additional level of regulation that bacteria switch on in poor conditions to enhance the survival rate, and this is a subject for our next study.

Figures, Tables and Schemes

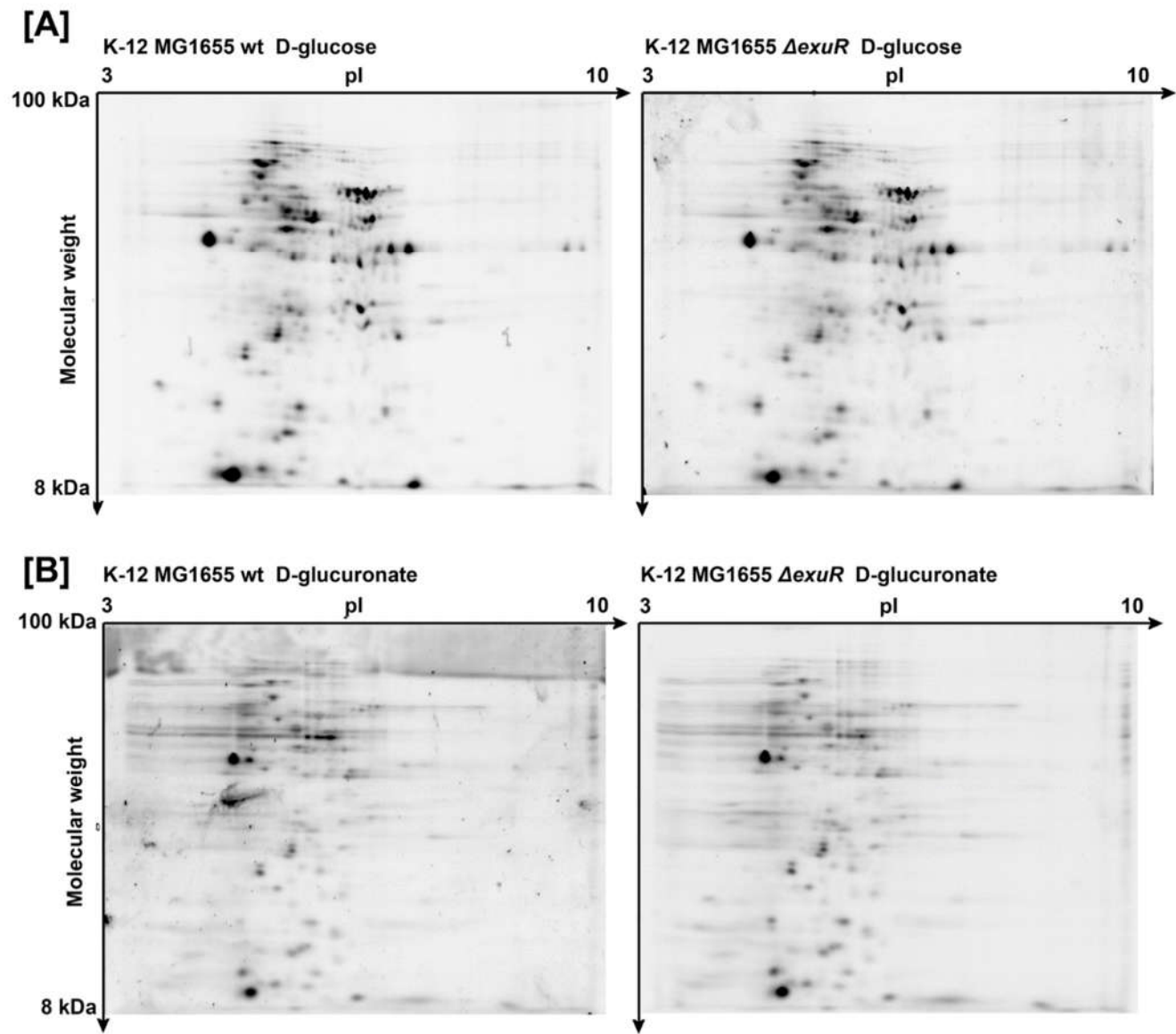


Figure 1. Proteomic maps of the wild type *E. coli* K-12 MG1655 and *E. coli* K-12 MG1655 Δ exuR during growth with D-glucose (a) and D-glucuronate (b). For each condition, 218 (a) and 160 (b) proteins were detected in both strains.

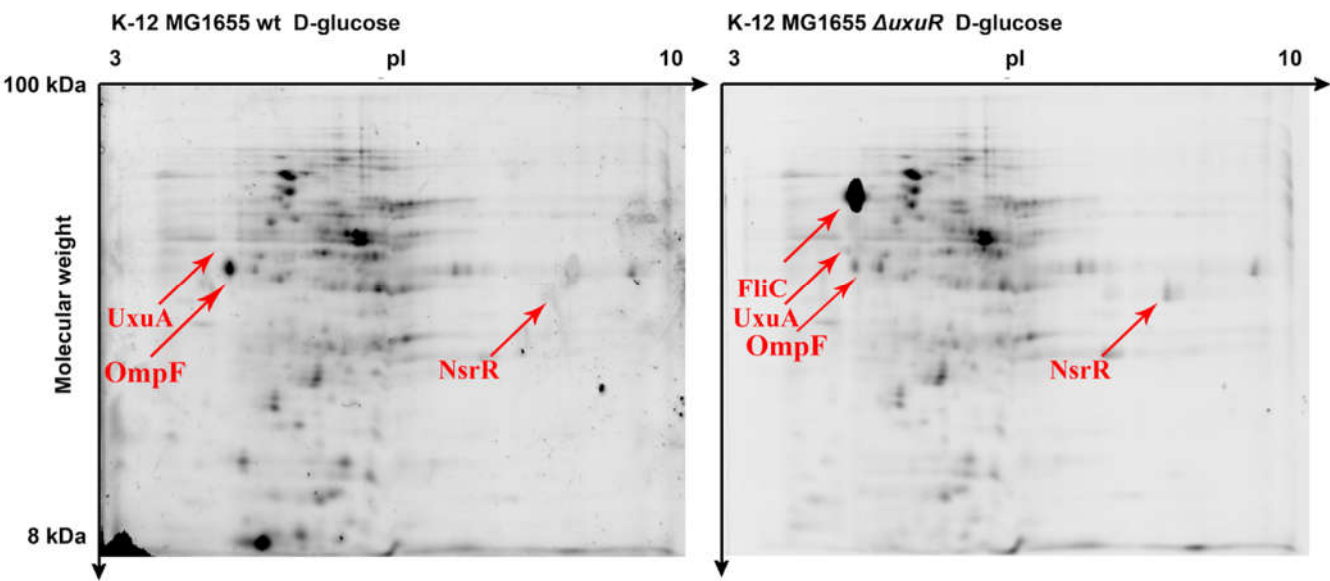


Figure 2. Proteomic maps of the wild type *E. coli* K-12 MG1655 and *E. coli* K-12 MG1655 $\Delta uxuR$ during growth with D-glucose. For D-glucuronate, gels are shown in Figure S2. 218 proteins were detected in both strains.

Table 1. Sequential separation of protein samples in the first direction.

	Voltage, V.	Time, min.
1	100	120
2	250	30
3	10000	120
4	10000	43000 Volt-time*

* Volt-time is an integral of voltage applied at the time of sample separation.

Table 2. Proteins with changed levels in the *E. coli* K-12 MG1655 Δ *uxuR* as compared to the wild type strain during growth on minimal medium with D-glucose as the main carbon source. Proteins with statistically significant scores are in bold. All proteins that were cut and analysed are shown in Supplementary Figure S1 and all proteins identified are listed in Supplementary Table 1.

Nº	Protein	Score	Function	Mw, Da	Effect of <i>uxuR</i> deletion
1	FliC	247	flagellar filament structural protein	51265	activated
2	UxuA	75	D-Mannonate dehydratase	44838	activated
3	GrcA	51	stress-induced alternate pyruvate formate-lyase subunit	14284	inhibited
4	YeiG	49	S-formylglutathione hydrolase	31308	inhibited
5	OmpF	48	Outer membrane porin F	39333	inhibited
6	NsrR	40	HTH-type transcriptional repressor	15583	activated
7	YdbK	33	pyruvate-flavodoxin oxidoreductase	128743	inhibited
8	EutM	27	putative ethanolamine catabolic microcompartment shell protein	9859	inhibited

Table 3. Proteins with changed levels in the *E. coli* K-12 MG1655 Δ *uxuR* as compared to the wild type strain during growth on minimal medium with D-glucuronate as the main carbon source. Proteins with statistically significant scores are in bold. All proteins that were cut and analysed are shown in Supplementary Figure S2 and all proteins identified are listed in Supplementary Table 1.

Nº	Protein	Score	Function	Mw, Da	Effect of <i>uxuR</i> deletion
1	CirA	202	Colicin I receptor	73850	inhibited
2	MglB	140	D-galactose-binding periplasmic protein	35690	activated
3	FumA	82	Fumarate hydratase class I, aerobic	60260	activated
4	HisJ	73	Histidine-binding periplasmic protein	28466	activated
5	RidA	70	2-iminobutanoate/2-iminopropanoate deaminase	13603	inhibited
6	OmpF	48	Outer membrane porin F	39333	inhibited
7	GrcA	39	stress-induced alternate pyruvate formate-lyase subunit	14259	inhibited

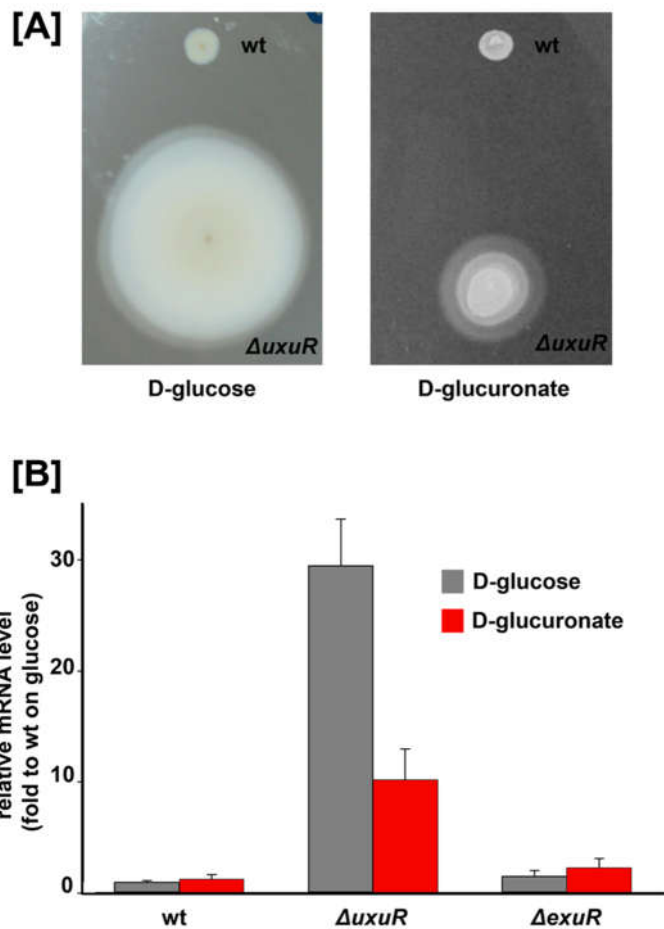


Figure 3. (a) Bacterial motility assay in 0.3% agar in the presence of 0.2% D-glucose or D-glucuronate. (b) Effects of UxuR and ExuR on *fliC* transcription. A panel represents qRT-PCR data for the *E. coli* K-12 MG1655 strain and its *uxuR* or *exuR* deletion mutants. No changes were detected in the *hns*-mRNA levels that were used as controls. mRNA levels are expressed relative to the parent strain during growth on glucose.

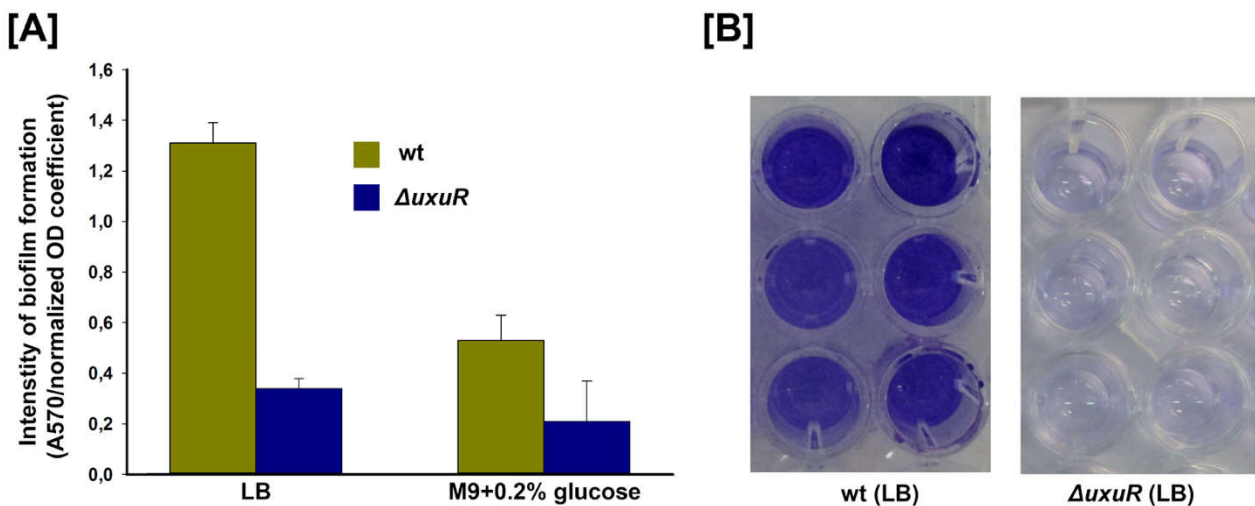


Figure 4. (a) Relative efficiency of biofilm formation of the wild type *E. coli* K-12 MG1655 strain and its *uxuR* deletion mutant after 48 hours of microaerobic growth on LB or M9 medium. (b) example of the staining intensity after 48 hours of microaerobic growth on LB.

3. Discussion

One of the main findings of this study is globally different effects of ExuR and UxuR earlier predicted to have similar functions, on the proteomes of *E. coli*. The absence of significant changes in the spectrum of proteins in the *exuR* deletion mutant in both tested conditions might suggest that this regulator does not play a major role in the control of the Ashwell pathway, as it was thought previously, at least, as a self-sufficient protein.

Its role was found to be rather uncertain already in the 1980s [11], and in line with this, we previously showed that *uxuR* and *exuR* deletions led to opposite effects on bacterial growth in the presence of D-glucuronate [12]. Deletion of *exuR* led to a slightly enhanced growth compared to the wild type, while deletion of *uxuR* resulted in dramatic inhibition of growth, suggesting the role of UxuR as an essential regulator of hexuronate metabolism that cannot normally function in its absence. Despite the fact that ExuR can form heterodimers with UxuR, causing derepression [12], it seems likely that by itself it does not affect expression of metabolically important genes and thus the proteomic maps of the *exuR* mutant in both conditions are identical to those of wild type. This is also consistent with our previous qRT-PCR and β -galactosidase data where effects of *exuR* deletion on its predicted targets were moderate [12].

In contrast, deletion of *uxuR* significantly altered the spectra of detected proteins during the *E. coli* growth both on glucose, a universal carbon source, and on glucuronate, substrate and intermediate of the Ashwell and Entner-Doudoroff pathways, but the changes were different. In the presence of glucose, the enzymes of sugar metabolism were affected, as well as proteins related to virulence and flagellar motion [22, 23]. In particular, significant activation of the structural flagellar protein FliC had been registered for the first time (Figure 1, Figure 3, Table 2), confirming the importance of UxuR for the control of the *E. coli* motility. Persistence of *E. coli* in the host organism suggests colonisation of epithelial cells in the intestine that is consistently reduced with activation of bacterial motility and is dependent on hexuronates that are controlled by UxuR [14, 15]. During growth with D-glucuronate, when metabolism mainly goes via the Ashwell pathway, no such effect had been observed (Table 3, Figure 3), in agreement with improved ability of bacteria to colonise the intestine [14-16].

Enhanced level of mannonate dehydratase synthesis (encoded by *uxuA*) in the K-12 MG1655 Δ *uxuR* can be considered as expected being explained by the loss of the UxuR repression at the *uxuAB* promoter [24]. Increased level of the NsrR transcription factor was far less predictable (Table 2). Hence the difference between the strains was not very significant (Score of 40), it deserves some attention because transcription factors are normally present in the cells in small amounts and thus are poorly detected in the proteomes. The *nsrR* gene does not belong to the UxuR regulon which is rather small [25, 26]. However, in some strains of *Salmonella enterica* the gene coding for NO reductase is located in the close proximity to *uxuR* (microbesonline.org), and if the carbon source changes to D-glucuronate, the Nac level also changes (Supplementary Table 1). Hence UxuR might somehow be involved in regulation of nitrogen metabolism. NsrR, in contrast, controls expression of 34 operons of different functionality, including five local (*dsdC*, *feaR*, *fhlA*, *norR*, *pdhR*) and at least one global (*lrp*) transcriptional regulator. According to the information in RegulonDB [25], the strongest inhibitory effect of NsrR was detected for just four genomic loci. Among them, two operons of nitrogen assimilation (*nrfABCDEFG* and *hcr-hcr-poxB-ltaE-ybjT*), the *ytfE* gene, with mutations leading to sensitivity of *E. coli* to nitric oxide [27, 28] and the *fliAZ-tyj* operon. *fliA* encodes for a σ -factor, controlling all flagellar genes, including *fliC*. Because of that, the enhanced levels of NsrR should inhibit transcription from *fliA* and, hence, *fliC*. But we observed the opposite effect. This might indicate that NsrR participates in the flagellin biogenesis, sustaining its production at an optimal level. However, the question about molecular mechanisms leading to accumulation of FliC in the mutant cells remains open. Another interesting question that still needs an answer is how a bacterial cell with the *uxuR* deletion decides whether to form a biofilm or not.

Metabolic networks in living organisms, even prokaryotic, are complex systems of biochemical reactions being regulated mostly by the physical and chemical conditions in the environment. From this point of view, carbon sources serve not only as a source of nutrition but also play key roles in bacterial adaptation to the environmental conditions. In the presence of D-glucuronate, metabolic switches led to changes in synthesis of hemotaxis-related D-galactose-binding periplasmic protein MglB and Colicin I receptor CirA (Table 3). The latter is a membrane receptor protein interacting with antimicrobial colicins 1A and 1B. Receptors of this type may also participate in the iron transport [29]. At present we can not provide a biological explanation for its inhibition; however, taking into account changes in production of two other transport-related proteins, HisJ and OmpF, we might assume that deficiency of nutrients in the media pushes on synthesis of one transport proteins and switches off the others, less needed in the current conditions. In line with this assumption, some enzymes were activated (like L-malate-hydrolyase FumA) and others were inhibited (2-iminobutanoate/2-iminopropanoate deaminase RidA) (Table 3).

Summarising, the comparative analysis of proteomic maps of the wild type *E. coli* K-12 MG1655 strain and its *uxuR* and *exuR* mutant derivatives suggests differential roles of their protein products in regulation of gene expression and, specifically, a complex network for UxuR. This transcription factor may affect not only production of enzymes and transporters of sugar metabolism but also bacterial motility, biofilm formation and, indirectly, iron transport and nitrogen metabolism.

4. Materials and Methods

Bacterial strains and cultivation conditions

Escherichia coli K-12 MG1655 wild type strain and its derivatives with deleted *uxuR* and *exuR* genes [12] were used for all experiments. To prepare samples for DIGE, 1 ml of overnight culture grown in LB was transferred to 250 ml of M9 medium containing 5% LB and 0,2% D-glucose or D-glucuronic acid as a primary carbon source, and then cultivated at 37°C for 4.5 hours ($OD_{650}=0.3-0.4$) under constant shaking. The cells were stopped with centrifugation at 5000 g, 4°C for 10 minutes.

Preparation of samples for DIGE

Cell pellets from 20 ml of culture were resuspended in 3 ml of buffer containing 2% Triton-X-100, 65 mM DTT, 10 mM EDTA, 20 mM Tris-HCl pH 8,0, and 15 mg of Protease Inhibitor Mini Tablets, EDTA-free (Thermo Fisher Scientific, USA). Cells were disrupted on the Sonic Dismembrator 550 (Thermo Fisher Scientific, USA) for 15 minutes at 35% intensity. Cell debris and ribosomal fraction were precipitated by ultracentrifugation at 213000 g, 4°C for 30 minutes. Proteins were precipitated with addition of 1:1 (V:V) of 20% TCA and 0,2% DTT in ice-cold acetone to supernatant, and the resulting mixture was then incubated at +4°C overnight. Denatured proteins were centrifuged at 20000 g, +4°C for 15 minutes. The pellet was washed 3 times with 0,2% DTT in ice-cold acetone following by 1 wash with the milliQ water, air dried and dissolved in 40µl of buffer containing 7M urea, 2M thiourea, 4% (W:V) CHAPS, 65 mM DTT, 20mM Tris-HCl, pH 8.5. Protein concentration was measured using Quick Start™ Bradford Protein Assay Kit 1 (BioRad, USA) and validated using SDS-PAGE.

Protein labelling

Samples were visualised using Lumiprobe 3Dye™ (USA). Dyes were dissolved in 98% dimethylformamide to 1mM concentration. A protein sample was stained with either Cy3 or Cy5 (0.4mM final concentration) and incubated in the dark at +4°C for 30 minutes. The staining reaction was stopped by adding 1 µl of 10mM lysine followed by 10 minutes incubation at +4°C in the dark. Then, the buffer containing 7M urea, 2M thiourea, 4% (W:V) CHAPS, 0.6% (V:V) ampholytes and 65mM DTT, was added to a final volume of

330 µl. Proteins isolated from samples to be compared were mixed and used for the 2D electrophoresis.

2D differential electrophoresis (DIGE)

Isoelectric focusing of proteins was made on the Protean i12 IEF system (BioRad, USA) using commercial 17 cm gels with the 3-10 pH gradient (pH 3-10 IPG strip, Bio-Rad, USA). The programme used for isoelectric focusing is shown in Table 1. Separation of proteins in the second direction according to their molecular weights was made using SDS-PAGE. After isoelectrofocusing, the IPG strip was incubated in the buffer containing 6M urea, 2% SDS, 20% glycerol, 10mM DTT, 0.5M Tris-HCl, pH8.8, followed by 20 minutes incubation in the same solution supplemented with 10mM iodoacetamide.

Electrophoresis was performed on the PROTEAN II xi 2-D Cell system (Bio-Rad, USA) using the Laemmli protocol [17]. Concentrating gel contained 4% acrylamide (acrylamide:methylene bis acrylamide =37.5:1), 125 mM Tris-HCl, pH 6.8, 0.1% SDS; 0.2% (V:V) TEMED and 0.1% (V:V) APS. Resolving gel contained 15% acrylamide (acrylamide:methylene bis acrylamide =37.5:1), 375 mM Tris-HCl, pH 8.8, 0.1% SDS; 0.2% (V:V) TEMED and 0.1% (V:V) APS. Gels were run in the standard tris-glycine buffer (25 mM Tris-HCl, pH 8.3, 0.192 M glycine, 0.1% SDS).

Proteins were visualized using ChemiDoc MP Imaging System (BioRad, USA) and Image Lab (BioRad, USA). Proteomes of the cells growing on different carbon sources or of the wild type and mutant cells were compared on one gel. All experiments were made at least in duplicates. For the *uxuR* deletion mutant, the experiment was repeated four times.

MALDI-TOF mass-spectrometry

Proteins were extracted from the gel in 150 µl 50% (V:V) acetone and 50% (V:V) 50 mM ammonium bicarbonate at 37°C (two times for 15 minutes) followed by dehydration in 100% acetonitrile. Then, 25 ng trypsin in 50 mM ammonium bicarbonate buffer was added, and the samples were incubated at 37°C for 16 hours. Then the supernatant was transferred to new tubes, and hydrolysate was either mixed 1:1 (V:V) with a solution containing 2% 2,5-dihydroxybenzoic acid in 50% acetonitrile and 3% trifluoroacetic acid, or mixed with 400 µl of 60% acetonitrile in 0.1% trifluoroacetic acid, vacuum dried at 45°C and dissolved in 20 µl of 30% acetonitrile in 0.1% trifluoroacetic acid.

Analysis was made on a MALDI-TOF / TOF (Ultraflex, Bruker Daltonik, Germany) equipped with the Nd:YAG laser in a reflector mode, m/z of 700-3500, 50 ppm ("Human Proteome" Facility) [18]; or on a MALDI-TOF / TOF (Rapiflex, Bruker Daltonik, Germany) equipped with the SmartBeam III laser in a reflector mode, m/z of 600-5000, 50 ppm (Skoltech Core Proteomics Facility). Spectrometer was calibrated with the Peptide Calibration Standard II and, additionally, by the trypsin autolysis peaks.

Proteins were identified using MASCOT (www.matrixscience.com) [19] based on the SwissProt database (www.uniprot.org). Candidate proteins were considered as confident if the score was higher than 49 ($p < 0,05$). All experiments were made at least in duplicates.

Biofilm and motility assays

To measure the intensity of biofilm formation, 10 µl of an overnight culture was used to inoculate a 96-well microtiter plate (REF 83.3924, Sarstedt, Germany) containing 90 µl of LB or M9+5%LB. The plate was incubated for 48 hours at 37°C in microaerobic conditions without shaking. Then, unattached cells were washed with phosphate buffer saline (PBS), while the remaining were fixed, dried and stained with 1% crystal violet as described in [20]. Each experiment was made at least with three independent cultures, in triplicate on each plate.

For motility assays, bacterial strains were grown in LB until late-log phase and then one microliter was placed onto a LB plate containing 0.3% agar (swimming motility plate).

The plates were incubated at 37°C for 4-6 hours, and motility zones from the point of inoculation were examined [21].

RNA extraction and quantitative PCR

RNA was extracted using TriZol reagent (Invitrogen, USA) according to the manufacturer's protocol and treated with the DNase I (New England Biolabs, USA) for 1 hour at 37°C followed by 10 minutes of inactivation at 70°C. RNA concentration was measured on a NanoDrop-1000 spectrometer (NanoDrop Technologies, USA), and quality was checked on a 4% polyacrylamide gel with 8M urea. Reverse transcription was made with the RevertAid M-MuLV reverse transcriptase (ThermoFisher Scientific, USA) and a gene specific primer fliC-R 5'-TTAGTACCGGTAGTGGCCTG-3'. Briefly, 1 µg of RNA was mixed with 4 pmol of the primer and heated for 10 minutes at 70°C. Then, 8 µl of the preheated master-mix was added containing 1x buffer (ThermoFisher Scientific, USA) and 2 µl dNTP mix (2.5mM each). The samples were chilled on ice for 2 minutes, then 40 units of the enzyme were added, and the mixture was further incubated for 40 minutes at 39°C. The reaction was stopped at 85°C for 5 minutes.

A DT-Lite thermocycler (DNA-Technology, Russia) and qPCR-HS mix (Evrogen, Russia) were used for quantitative PCR (qRT-PCR). The second primer was fliC-F 5-TCTGTCTTCTGGCTTGCCTA-3'. The *hns* gene coding for the nucleoid protein was used as a normalization control [12]. No PCR products were detected in negative controls in the absence of reverse transcriptase. Data obtained from at least three biological samples and analyzed in three statistical replicates were calculated by the ΔC_t method. The error bars indicate the standard deviations of corresponding mean values.

Supplementary Materials: Figure S1: Proteomic maps of the *E. coli* K-12 MG1655 wild type and its *uxuR* deletion mutant during growth with D-glucose; Figure S2: Proteomic maps of the *E. coli* K-12 MG1655 wild type and its *uxuR* deletion mutant during growth with D-glucuronate; Figure S3: Proteomic maps of the *E. coli* K-12 MG1655 wild type during growth with D-glucose or D-glucuronate; Figure S4: Series of experiments on the biofilm formation by the *uxuR* deletion mutant on minimal medium; Table S1: Proteins detected by mass-spectrometry in different conditions.

Author Contributions: Conceptualization, M.S.G., M.N.T., O.N.O., S.V.T and A.D.N.; methodology, M.S.F., O.S.K. and T.A.B.; validation, T.A.B. and O.S.K.; formal analysis, M.S.F. and S.V.T.; investigation, T.A.B., M.S.F., O.S.K. and M.N.T.; resources, A.D.N and O.N.O.; data curation, T.A.B., M.S.F., O.S.K. and M.N.T.; writing—original draft preparation, M.N.T. and S.V.T.; writing—review and editing, M.S.G. and O.N.O.; visualization, M.N.T. and T.A.B.; supervision, M.N.T., M.S.G. and S.V.T.; project administration, S.V.T. and A.D.N.; funding acquisition, A.D.N, M.S.G. All authors have read and agreed to the published version of the manuscript.

Funding: This research was funded by RSF 18-14-00322 (ADN, proteomic analysis) and 18-14-00358 (MNT and MSG, physiology experiments).

Acknowledgments: Mass-spectrometry was made by the “Human Proteome” facility in the Institute of Biomedical Chemistry named after V.N. Orekhovich and by the Skoltech Core Proteomics Facility. We thank Anna Potapova for the help with qRT-PCR experiments.

Conflicts of Interest: The authors declare no conflict of interest. The funders had no role in the design of the study; in the collection, analyses, or interpretation of data; in the writing of the manuscript; or in the decision to publish the results.

References

1. Suvorova, I.A.; Tutukina, M.N.; Ravcheev, D.A.; Rodionov, D.A., Ozoline; O.N.; Gelfand, M.S. Comparative genomic analysis of the hexuronate metabolism genes and their regulation in gammaproteobacteria, *J Bacteriol* **2011**, *193*, 3956–3963, doi: 10.1128/jb.00277-11.
2. Hugouvieux-Cotte-Pattat, N.; Robert-Baudouy, J. Isolation of fusions between the lac genes and several genes of the exu regulon: analysis of their regulation, determination of the transcription direction of the *uxaC-uxaA* operon, in *Escherichia coli* K-12. *Mol Gen Genet* **1981**, *182*:279–287.
3. Mata-Gilsinger, M.; Ritzenthaler, P.; Blanco, C. Characterization of the operator sites of the *exu* regulon in *Escherichia coli* K-12 by operator-constitutive mutations and repressor titration. *Genetics* **1983**, *105*:829–842.

4. Ritzenthaler, P.; Mata-Gilsinger, M. Multiple regulation involved in the expression of the *uxuR* regulatory gene in *Escherichia coli* K-12. *Mol Gen Genet* **1983**, 189:351–354.
5. Nemoz, G.; Robert-Baudouy, J.; Stoeber, F. Physiological and genetic regulation of the aldohexuronate transport system in *Escherichia coli*. *J Bacteriol* **1976**, 127:706–718.
6. Portulier, R.; Robert-Baudouy, J.; Stoeber, F. Regulation of *Escherichia coli* K-12 hexuronate system genes: *exu* regulon. *J Bacteriol* **1980**, 143:1095–1107.
7. Rodionov, DA.; Mironov, AA.; Rakhmaninova, AB.; Gelfand, MS. Transcriptional regulation of transport and utilization systems for hexuronides, hexuronates and hexonates in gamma purple bacteria. *Mol Microbiol* **2000**, 38:673–683.
8. Rodionov, DA.; Gelfand, MS.; Hugouvieux-Cotte-Pattat, N. Comparative genomics of the KdgR regulon in *Erwinia chrysanthemi* 3937 and other gamma-proteobacteria, *Microbiology* **2004**, 150: 3571–3590, doi: 10.1099/mic.0.27041-0.
9. Bates Utz, C.; Nguyen, AB.; Smalley, DJ.; Anderson, AB.; Conway, T. GntP is the *Escherichia coli* Fructuronic acid transporter and belongs to the UxuR regulon. *J bacteriol* **2004**, 186, 7690–6, doi: 10.1128/JB.186.22.7690-7696.2004.
10. Blanco, C.; Ritzenthaler, P.; Mata-Gilsinger, M. Negative dominant mutations of the *uidR* gene in *Escherichia coli*: genetic proof for a cooperative regulation of *uidA* expression., *Genetics*, **1986**, 112, 173–182.
11. Ritzenthaler, P.; Blanco, C.; Mata-Gilsinger, M. Genetic analysis of *uxuR* and *exuR* genes: evidence for ExuR and UxuR monomer repressors interactions., *Mol gen genet* **1985**, 507–11, doi: <https://doi.org/10.1007/BF00330766>.
12. Tutukina, MN.; Potapova, AV.; Cole, JA.; Ozoline, ON. Control of hexuronate metabolism in *Escherichia coli* by the two interdependent regulators, ExuR and UxuR: derepression by heterodimer formation, *Microbiology* **2016**, 162, 1220–1231, doi: 10.1099/mic.0.000297.
13. Peekhaus, N.; and Conway, T. What's for Dinner?: Entner-Doudoroff Metabolism in *Escherichia coli*, *J Bacteriol* **1998**, 180, 3495–3502, doi: 10.1128/JB.180.14.3495-3502.1998.
14. Chang D-E.; Smalley, DJ.; Tucker, DL.; Leatham, MP.; Norris, WE.; Stevenson, SJ.; Anderson, AB.; Grissom, JE.; Laux, DC.; Cohen, PS.; Conway, T. Carbon nutrition of *Escherichia coli* in the mouse intestine. *Proc Natl Acad Sci U S A* **2004**, 101:7427–7432.
15. Fabich, AJ.; Jones, SA.; Chowdhury, FZ.; Cernosek, A.; Anderson, A.; Smalley, D.; McHargue, JW.; Hightower, GA.; Smith, JT.; Autieri, SM.; Leatham, MP.; Lins, JJ.; Allen, RL.; Laux, DC.; Cohen, PS.; Conway, T. Comparison of carbon nutrition for pathogenic and commensal *Escherichia coli* strains in the mouse intestine. *Infect Immun* **2008**, 76:1143–1152.
16. Jimenez, A.G.; Ellermann, M.; Abbott, W.; Sperandio, V. Diet-derived galacturonic acid regulates virulence and intestinal colonization in enterohaemorrhagic *Escherichia coli* and *Citrobacter rodentium*. *Nat Microbiol* **2020**, 5, 368–378 (2020). <https://doi.org/10.1038/s41564-019-0641-0>
17. Laemmli, U.K. Cleavage of Structural Proteins during the Assembly of the Head of Bacteriophage T4, *Nature* **1970**, 227, 680–685.
18. Andreeva, A.M.; Vasiliev, A.S.; Toropygin, I.Yu.; Garina, D.V.; Lamash, N.; Filippova, A. Involvement of apolipoprotein A in maintaining tissue fluid balance in goldfish *Carassius auratus*, *Fish Physiol Biochem* **2019**, 45, 1717–1730, doi: 10.1007/s10695-019-00662-1.
19. Perkins, D.N., Pappin, D.J., Creasy, D.M., and Cottrell, J.S. (1999) Probability-based protein identification by searching sequence databases using mass spectrometry data, *Electrophoresis*, **20**, 3551–3567, doi: 10.1002/(SICI)1522-2683(19991201)20:18<3551::AID-ELPS3551>3.0.CO;2-2.
20. Pratt, LA.; Kolter, R. Genetic analysis of *Escherichia coli* biofilm formation: roles of flagella, motility, chemotaxis and type I pili. *Mol microbiol* **1998**, 30, 285–293.
21. Fuentes, DN.; Calderón, PF.; Acuña, LG.; Rodas, PI.; Paredes-Sabja, D.; Fuentes, JA.; Gil, F.; Calderón, IL. Motility modulation by the small non-coding RNA SroC in *Salmonella Typhimurium*. *FEMS Microbiol Lett* **2015** 362(17):fnv135. doi: 10.1093/femsle/fnv135.
22. Sweeney, N.J.; Laux, D.C.; Cohen, P.S. *Escherichia coli* F-18 and *E. coli* K-12 *eda* mutants do not colonize the streptomycin-treated mouse large intestine, *Infect Immun* **1998**, 64, 3504–3511, doi: 10.1128/IAI.64.9.3504-3511.1996.
23. Patra, T.; Koley, H.; Ramamurthy, T.; Ghose, AC.; Nandy, RK. The Entner-Doudoroff pathway is obligatory for gluconate utilization and contributes to the pathogenicity of *Vibrio cholerae*. *J Bacteriol* **2012**, 194(13):3377–85. doi: 10.1128/JB.06379-11.
24. Blanco, C.; Ritzenthaler, P.; Kolb, A. The regulatory region of the *uxuAB* operon in *Escherichia coli* K12. *Mol Gen Genet* **1986**, 202(1):112–9. doi: 10.1007/BF00330526.
25. Gama-Castro, S.; Salgado, H.; Santos-Zavaleta, A.; Ledezma-Tejeda, D.; Muñoz-Rascado, L.; García-Sotelo, JS.; Alquicira-Hernández, K.; Martínez-Flores, I.; Pannier, L.; Castro-Mondragón, JA.; Medina-Rivera, A.; Solano-Lira, H.; Bonavides-Martínez, C.; Pérez-Rueda, E.; Alquicira-Hernández, S.; Porrón-Sotelo, L.; López-Fuentes, A.; Hernández-Koutoucheva, A.; Del Moral-Chávez, V.; Rinaldi, F.; Collado-Vides, J. RegulonDB version 9.0: high-level integration of gene regulation, coexpression, motif clustering and beyond. *Nucleic Acids Res* **2016**, 44:D133–143.
26. Shimada, T.; Ogasawara, H.; Ishihama, A. Single-target regulators form a minor group of transcription factors in *Escherichia coli* K-12. *Nucleic Acids Res* **2018**, 46(8):3921–3936. doi: 10.1093/nar/gky138.
27. Vine, CE.; Justino, MC.; Saraiva, LM.; Cole, J. Detection by whole genome microarrays of a spontaneous 126-gene deletion during construction of a *ytfE* mutant: confirmation that a *ytfE* mutation results in loss of repair of iron-sulfur centres in proteins damaged by oxidative or nitrosative stress. *J Microbiol Methods* **2010**, 81(1):77–9. doi: 10.1016/j.mimet.2010.01.023.
28. Cole, JA. Anaerobic bacterial response to nitric oxide stress: Widespread misconceptions and physiologically relevant responses. *Mol Microbiol* **2021**, 116(1):29–40. doi: 10.1111/mmi.14713.

-
29. Tiel-Menkveld, G.J.V.; Mentjox-Vervuurt, J.M.; Oudega, B.; Graaf, F.K. de Siderophore production by *Enterobacter cloacae* and a common receptor protein for the uptake of aerobactin and cloacin DF13. *J Bacteriol*, **1982**, 150, 490–497.